

New insights for testing linearity and complexity with surrogates: a Recurrence Plot approach

A. Carrión and R. Miralles

Abstract

The detection and characterization of non-linearities in temporal series is a hot topic in some disciplines such as nondestructive testing of materials, bioacoustics and biomedical research domains. This is a complex interdisciplinary field where many different researchers are striving to achieve better and more sophisticated techniques. In this scenario, the search for new perspectives that can explain and unify some of the theories is of key importance. Recurrence Plots (RPs) and Recurrence Quantification Analysis (RQA) can play such a role. In this work, we show how RPs can be used to design tests for non-linear detection and characterization of complexity. The proposed tests are less parameter dependent and more robust than some of the traditional discriminating measures. We also illustrate the applicability of the proposed algorithms in simulations and real-world signals such as the analysis of anomalies in the voice production of mammals.

1 Introduction

Detecting non-linearities and complexity in time signals can be used in many situations as an indicator of changes in the underlying dynamical system that is responsible for the generation of those signals. In some disciplines, the study of these phenomena has not been addressed and it is a common practice to model these processes using suboptimal, but mathematically, tractable models. However, an appropriate detection and characterization of the non-linear and deterministic nature

A. Carrión

Instituto de Telecomunicación y Aplicaciones Multimedia (iTEAM), Universitat Politècnica de València, Camino de Vera S/N, 46022, Valencia, Spain e-mail: alcarga4@upv.es

R. Miralles

Instituto de Telecomunicación y Aplicaciones Multimedia (iTEAM), Universitat Politècnica de València, Camino de Vera S/N, 46022, Valencia, Spain e-mail: rmiralle@com.upv.es

of the signal can convey important information in a large number of situations such as: early detection of epileptic symptoms with EEG signals [1], non-linear phenomena in mammalian voice production [2], stock market predictability [3], river flow discharge rates [4], etc.

Many authors have worked on different techniques to detect and characterize non-linearities in time series. One of the most commonly used methods is the Monte-Carlo approach, namely the surrogate data bootstrapping method. This approach is based on the computation of an ensemble of surrogates which are representative realizations of the null hypothesis under study. A statistical measure is computed for the original time series and the surrogates. If the statistic is significantly different from the values obtained for the surrogate set, the null hypothesis can be rejected. Therefore, there are three major aspects of the surrogate data method that need to be considered: 1) the exact definition of the null hypothesis, 2) the realization of the null hypothesis, and 3) the test statistic.

In the literature, different kinds of surrogate generation algorithms can be found based on the null hypothesis under study: stationarity/non-stationarity [5], determinism/randomness [6], linearity/non-linearity [7, 8], chaos [9], etc. A surrogate data generation algorithm for testing fluctuations and trends in data is the Small-shuffle surrogate algorithm (SSS) [10], surrogate data generation algorithms for testing pseudo-periodic or oscillating time series are the pseudoperiodic surrogates (PPS) [11] and the twin surrogates (TS) [12, 13], and surrogate data generation algorithms for testing linearity include the well-known Amplitude Adjusted Fourier Transform (AAFT) [7] and its improved version, the iterative Amplitude Adjusted Fourier Transform (iAAFT) [14]. In each analysis, different statistical measures are applied to quantify the differences between the original data and the surrogates. Some of the methods applied in linear analysis are Kaplans δ - ε [15], Deterministic Versus Stochastic plots [16], or Delay Vector Variance (DVV) [17].

The use of the RP may have an important role in the signal modality characterization framework. In this work, we analyze how this visualization tool not only can be applied for the generation of surrogate data but also for the quantification of statistical differences between the original data and the surrogate data. We have mainly focused on two main features of signal modality: the characterization of the linear/non-linear nature of a signal and its complexity.

To explain these ideas, the following definitions are used throughout this work. We can compute the phase-space representation of a given N -point signal x_t for an embedding dimension (m) and a time lag (τ) by computing the Delay Vectors (DVs) using Eq. (1) [18]:

$$\mathbf{x}(i) = [x_{i-m\cdot\tau}, x_{i-(m-1)\cdot\tau}, \dots, x_{i-\tau}] \quad (1)$$

Every delay vector has a corresponding target which is basically the next sample x_i [19]. The proper selection of τ and m is crucial in the following analysis since it affects the correct representation of the data evolution in time. A common approach to determine the time lag is the one proposed by [20], which uses the first local minimum of the time-delayed mutual information as a reasonable value for τ . The

selection of the minimum embedding dimension m is based on the false nearest neighbor algorithm proposed in [21, 22].

RPs are calculated using Eq. (2) [23]:

$$RP_{i,j} = \begin{cases} 1 & \text{if } \|\mathbf{x}(i) - \mathbf{x}(j)\| \leq \varepsilon \\ 0 & \text{otherwise} \end{cases} \quad (2)$$

where $\|\cdot\|$ is the Euclidean norm and the parameter ε is a threshold distance (or recurrence threshold). The quantification of RPs can be done by means of RQA.

The remainder of this work is structured as follows. In Section 2, we present a selection of surrogate techniques that can be applied to test the linear/non-linear nature of real signals that have a non-stationary behaviour. In this section, we also present a new surrogate technique to test the presence of high complexity in oscillatory signals. In Section 3, we illustrate how new discriminating measures for non-linear statistical tests can be designed using RQA. Section 4 presents some examples of signal modality characterization with both simulated and real signals. Finally, we present our conclusions in Section 5.

2 Surrogate techniques

Theiler et al. [7] introduced the concept of ‘surrogate data’, which has been extensively used in the context of statistical non-linearity testing. A surrogate time series (or surrogate for short) is generated as a realization of the null hypothesis under study. Thus, given an original signal, realizations of this data must be generated by modifying only the desired characteristic of the signal that is being tested, while the rest of the characteristics remain the same. Care must be taken when using surrogate data to ensure that the statistical differences come from the desired characteristic and not from an undesired one, such as a failure of the surrogate algorithm to mimic non-stationary data. Choosing a surrogate technique that does not mimic these fluctuations or that changes the statistical distribution may lead to false positives.

Below we next present two techniques for the generation of surrogates that will be used later in a statistical analysis based on RQA. The first technique is used to detect the presence of non-linearities; whereas the second technique uses RP concepts to generate surrogates that are valid for testing high complexity in short oscillatory signals.

2.1 Surrogates for testing non-linearity

One of the key issues in signal processing is the definition of a linear signal. The standard definition is that it is a signal that is generated by a Gaussian linear stochastic process. Based on this definition, the null hypothesis refers to the properties of

any AR-model that is driven by white noise. Since any AR-model can be described by its amplitude spectrum (and thus the phase spectrum is irrelevant), most surrogate data generation algorithms for testing linearity are based on a phase spectrum randomization. The most common established method for generating constrained surrogates is the Iterative Amplitude Adjusted Fourier Transform (iAAFT) [14].

Let x_t be the original time series, s_k the sorted version of x_t , and X_k the Fourier transform of the original data series. The original iAAFT algorithm is based on the following steps:

1. Make a random permutation of the time samples of the original time series x_t , namely r_t .
2. Compute the phase spectrum of r_t , namely ϕ_k .
3. Compute the Inverse Fourier Transform of $\{|X_k| \cdot \exp(j\phi_k)\}$, namely c_t .
4. Obtain a new version of the time series r_t by rank-ordering (sort in increasing order) c_t so as to match s_k .
5. Repeat steps 2-4 until the discrepancy between $|X_k|$ and the amplitude spectrum of r_t is lower than a chosen tolerance.

This iterative algorithm has been shown to converge after a finite number of steps [14]. Each initial random permutation gives a different output surrogate data r_t with identical signal distribution and approximately identical amplitude spectra as the original signal.

The original iAAFT method has recently been refined to not only retain the signal distribution and amplitude spectrum of the original time series but also to retain the local mean and variance of the original time series [24]. This new approach uses a wavelet transform to preserve the behavior in the time-frequency plane. It makes this new technique very suitable for non-stationary signals whose time-changing properties would be destroyed using the original iAAFT algorithm.

Let x_t be the N -point original time series and s_k the sorted version; x_t is decomposed in J scales, where $N = 2^J$, $j = 1, 2, \dots, J$. The WiAAFT algorithm can be summarized as follows:

1. Compute the Maximal Overlap Discrete Wavelet Transform (MODWT) of the original time series x_t using a high number of vanishing moments to deal with any potential non-stationarity in the series [25]. The result is a vector of wavelet detail coefficients, c_j , at each scale j .
2. Apply the iAAFT algorithm to each c_j to generate a constrained realization of the original detail coefficients, c'_j , preserving the original values and their periodicity.
3. Transpose c'_j so that the first detail coefficient in the transposed case is the last one in the new variant, c''_j .

4. Find the best match in each scale between c_j and the two variants, c'_j and c''_j , by circularly rotating until an error function is minimized. In this work, least-squares algorithm is used. This means that the positions with high energies in the original data are mimicked in the surrogates.
5. Invert the MODWT (using the original approximation coefficients) to yield a surrogate dataset, w_t .
6. Perform rank-ordering (sort in increasing order) to w_t so as to match s_t .
7. Use the new time series w_t as the initialization of the described iAAFT algorithm.

Fig. 3 compares the surrogate data computed with the original iAAFT algorithm and the new WiAAFT for a heart-rate variability signal (HRV) that is recorded during a meditation session. HRV signals are widely used to analyze human health; however, from the signal processing point of view, one of the main drawbacks is the presence of many artifacts or temporal changes in the recorded time series due to different factors such as patient motion, eye blinking, etc. that may lead to non-stationarities. The blue line represents the original time series. The green line corresponds to the surrogate data that is computed using the iAAFT. Note that the iAAFT has almost destroyed the temporal structure of the original signal. The red line plots the surrogate data that is computed with the WiAAFT algorithm. Even though, this new surrogate data is still a random realization compared with the original data, it greatly preserves the time evolution of the original data. The WiAAFT algorithm has been observed to yield superior results when testing for linearity.

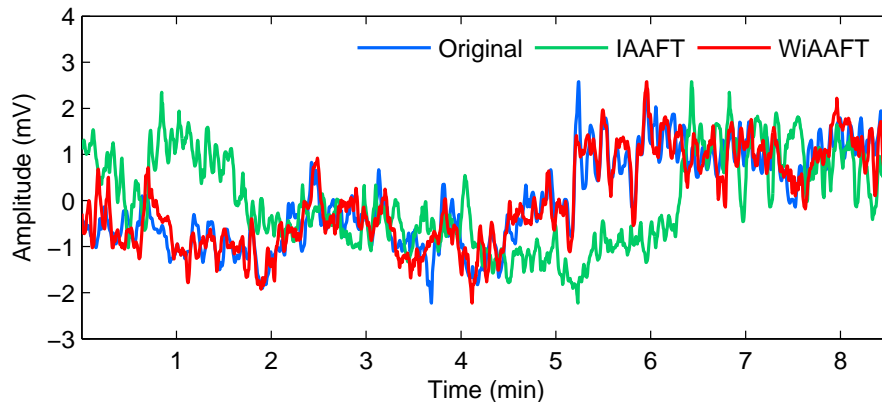


Fig. 1 Comparison between two surrogate data generation algorithms (iAAFT and WiAAFT) for a heart-rate variability signal (HRV) recorded during a meditation session. The blue line represents the original non-stationary signal; the green line represents the surrogate data computed with the iAAFT; and the red line corresponds to the surrogate data computed with the WiAAFT.

2.2 Pseudo-Periodic Twin Surrogates (PPTS)

Oscillatory signals can often be found in the solution of real-world problems. Sometimes these signals have a high complexity in the oscillations, which may indicate the presence of non-linearities. Some examples are: the study of biphonation, sub-harmonics or other pathologies in animal sounds [26], the study of non-linearities in ultrasonic signals [27], etc. In most of these problems, conventional surrogates have a limited use, mainly due to the finite duration of the events that need to be analyzed and due to the sensitivity that needs to be achieved. Some of the techniques that rely on the Fourier Transform require long data series, and therefore, specific algorithms for the generation of surrogates in short-length oscillating data have to be designed.

In the literature, there are several methods that preserve the higher order moments for the surrogate generation of oscillatory signals. The most representative methods for this work are the pseudoperiodic surrogates (PPS) method [11], the twin surrogates (TS) method [12, 13], and the pseudoperiodic twin surrogate (PPTS) method [28]. The PPTS method is a combination of the PPS and the TS which allows tests to be designed in order to check the null hypothesis that the observed time series is a quasi-periodic signal obtained as the sum of sinusoids with incommensurate frequencies.

The PPTS algorithm uses the phase space and RP concepts to obtain the surrogates. This is achieved by employing the idea of jumping among twin points in the same way that the TS algorithm does. Twin points are points that are neighbors, $\|\mathbf{x}(i) - \mathbf{x}(j)\| < \varepsilon_{TP}$, and they also share the same neighborhood $R_{i,l} = R_{j,l} \forall l$. Twin points are indistinguishable with respect to their neighborhoods, but they generally have different pasts and, more importantly, different futures. We can generate surrogates by changing the structures in the RP consistently with those produced by the underlying dynamic system. Jumping among twin points produces surrogates with RP representations that are very similar to the RP representation of the original signal if the time signal is periodic or quasi-periodic (similar futures). In contrast, jumping among twin points produces surrogates with RP representations that are quite different if the time signal is chaotic.

Unfortunately, jumping among twin points is not always enough to generate surrogates that allow the confidence level for null test rejection to be established. Additionally, there are some practical implementation problems with the TS algorithm for short time series (such as the limited number of twins [13]). Thus, the PPTS algorithm uses a second randomization technique. This technique consists of moving from point to point in the phase space in accordance with a probability that is inversely proportional to the distance between the two points (using Eq. (3) as is done in the PPS algorithm [11]). The proposed PPTS algorithm is summarized as follows:

1. Compute the RP of the original signal using Eq. (2), with an appropriate choice of ε , denoted by ε_{TP} , and identify the twin points ($R_{i,l} = R_{j,l} \forall l$).

The choice of ε_{TP} is not crucial for the PPTS; it has been shown in [12] that a choice of ε_{TP} corresponding to 5% -10% of black points in the RP is appropriate.

2. Randomly choose an initial condition i_0 and make $i = i_0$. Initialize $n = 1$.
3. If there is a twin point for $\mathbf{x}(i)$, make the next point of the surrogate $\mathbf{x}_s(n) = \mathbf{x}(j)$, where j is randomly chosen among the twin points with the probability $1/T$ (T is the number of twin points for the state $\mathbf{x}(i)$). Let $i = j$ and $n = n + 1$.
4. For $\mathbf{x}(i)$, choose a neighbour $\mathbf{x}(j)$ from all of the elements of the phase space representation ($j = m \cdot \tau, \dots, N - 1$) with probability

$$Prob(\mathbf{x}(j)) \propto \exp \frac{-\|\mathbf{x}(i) - \mathbf{x}(j)\|}{\rho} \quad (3)$$

where ρ is the noise radius studied in [11]. Make the next point of the surrogate $\mathbf{x}_s(n) = \mathbf{x}(j)$. Let $i = j$ and $n = n + 1$.

5. Repeat from Step (3) until $n = N$.

The surrogate is formed from the first scalar component of $\mathbf{x}_s(n)$.

The proposed PPTS algorithm generates surrogates that are very similar to the original signal as long as the original signal is periodic or quasi-periodic. When the original signal deviates from a periodic or quasi-periodic oscillation, the PPTS generates surrogates that have a RP matrix that is quite different while still preserving the approximate phase-space shape of the original signal. Thus, these surrogates are appropriate for testing the null hypothesis that the observed time series is consistent with a quasi-periodic orbit. This is illustrated in the following example.

2.2.1 Example

Consider the following signals: a quasi-periodic time series composed of the sum of two sinusoids with incommensurate frequencies and a Rössler chaotic time series [29].

The quasi-periodic signal was generated as given by:

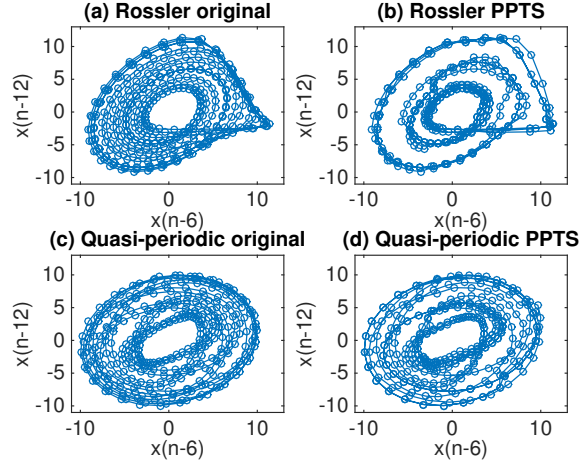
$$x(t) = 8 \cdot \sin(2 \cdot \pi \cdot f_1 \cdot t) + 4 \cdot \sin(2 \cdot \pi \cdot f_2 \cdot t) \quad (4)$$

where $f_1 = \sqrt{3}$ Hz, $f_2 = \sqrt{5}$ Hz. The discrete time series version x_n^{quasi} is obtained using a sample period of $\Delta t = 0.02$ s. We only generate 400 samples of this signal.

The Rössler signal is generated as given by:

$$\begin{cases} \dot{x} = -y - z \\ \dot{y} = x + ay \\ \dot{z} = b + z(x - c) \end{cases} \quad (5)$$

Fig. 2 (a) Phase-space reconstruction of the Rössler attractor; (b) Phase space reconstruction of the PPTS for the Rössler attractor; (c) Phase space reconstruction of the quasi-periodic time series; (d) Phase space reconstruction of the PPTS for the quasi-periodic time series. The PPTS were computed with ε_{TP} corresponding to 10% of black points in the RP and a $\rho = 0.25$.



with the initial conditions $x(0) = y(0) = z(0) = 0.1$, $a = 0.2$, $b = 0.2$, $c = 5.7$ (chaotic state) and a sampling time of $\Delta t_s = 0.2$. The system was integrated 1400 times using the Matlab ODE solver ODE45, and the time series $x_n^{Rössler}$ was obtained from the x component after discarding the first 1000 data points to avoid transient states (again, only 400 data points were used).

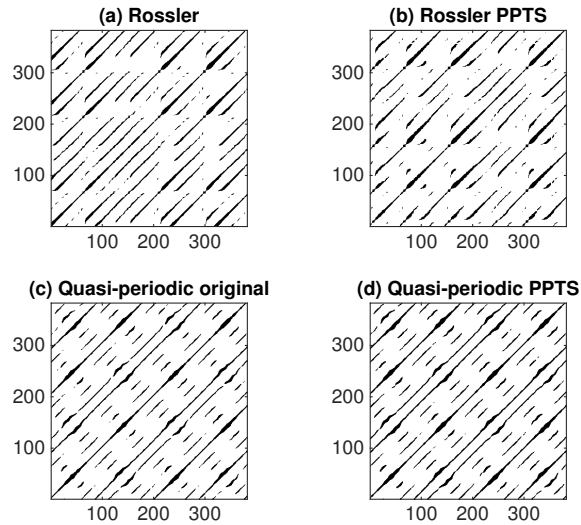
Fig. 2 illustrates the phase-space reconstruction (with $m = 2$ and $\tau = 6$) of the following: (a) the original Rössler time series, and (b) the PPTS. From the comparison of (a) and (b), it can be observed how the proposed PPTS algorithm achieves a phase-space representation that removes most of the details that indicate chaos (the large number of trajectories that run arbitrarily close together) while at the same time preserving the shape of the original time series. In the same way, the panels (c) and (d) show the phase-space reconstruction of the original quasi-periodic time series and the phase-space reconstruction of the PPTS of the quasi-periodic signal. In this situation both the phase-space diagram of the quasi-periodic and its PPTS look very similar.

All of these details are captured and represented in the structures of the RPs (see Fig. 3). The appropriate metrics for testing using the PPTS (or some of the other surrogates presented) can then be obtained by means of the RQA. This idea, which is detailed in the following section, allows us to create tests to distinguish between oscillatory signals with different complex patterns of amplitude modulation.

3 Discriminating non-linearity tests and statistics based on Recurrence Plots

In order to test the null hypothesis of linearity, a statistical discriminating measure has to be performed on both the original data and the surrogates. Many different

Fig. 3 (a) RP representation of the Rössler attractor; (b) RP representation of the PPTS for the Rössler attractor; (c) RP representation of the quasi-periodic time series; (d) RP representation of the PPTS for the quasi-periodic time series. The PPTS were computed with ε_{TP} corresponding to 10% of black points in the RP and a $\rho = 0.25$.



techniques and statistical tests have been suggested for this purpose. Some of the discriminating statistics are based on computing Lyapunov exponents, return maps, or some other graphs or functions that are representative of the topology of the underlying dynamics. The computation of these functions can be quite complex in real-world signals. As a result of this difficulty, a large number of techniques that compute a much more simple graphical representation of the underlying system have been developed. Some of the most cited methods are Deterministic versus Stochastic plots [16], Kaplans $\delta - \varepsilon$ [15], correlation exponent [30], or Delay Vector Variance (DVV) [17].

All of these methods introduce the DV \mathbf{x}_i presented above (Eq. 1), as well as the concept of the target of the DV x_i (basically, the next sample). The idea underpinning these methods is that the study of the locality of the unknown models (which maps the DVs onto their corresponding targets) when combined with the method of the surrogates provides information of the non-linear behaviour of the underlying process. The degree of locality of a time series is closely related to the distribution of the nearest neighbour points; however, each method analyzes the degree of locality using different approaches: the mean of the targets, the variance of the targets, the prediction error, etc. Even though these studies are very thorough, none of them exploit the advantages of RP, and thus, the advantages of RQA.

RPs can help greatly in the design of robust and less parameter dependent tests for non-linearity detection. In the following, a detailed analysis of one of the above-mentioned methods is done in order to further understand the motivation of this new approach and its potential.

3.1 Reformulation of the DVV using RPs

The delay vector variance (DVV) method is a phase-space based technique that examines the deterministic nature of a time series and that provides information of the non-linear behavior of the underlying process when it is combined with the method of surrogate data.

The DVV method can be summarized as follows [17].

1. Compute the optimal embedding parameters, m and τ , and generate the delay vectors (DVs) using Eq. 1. Every DV, $\mathbf{x}(i)$, has a corresponding target, namely the next sample x_i .
2. Compute the mean, μ_d , and the standard deviation, σ_d , over all pairwise Euclidean distances between DVs, $\|\mathbf{x}(i) - \mathbf{x}(j)\| (i \neq j)$.
3. Generate the sets $\Omega_k(r_d)$ such that $\Omega_k(r_d) = \{\mathbf{x}(i) \mid \|\mathbf{x}(k) - \mathbf{x}(i)\| \leq r_d\}$ (sets that consist of all DVs that lie closer to $\mathbf{x}(k)$ than a certain distance r_d , taken from the interval $[\max\{0, \mu_d - n_d \sigma_d\}]$). For example, generate N_{rv} uniformly spaced distances, where n_d is a parameter controlling the span over which to perform the DVV analysis.
4. Compute the variance of the corresponding targets, $\sigma_k^2(r_d)$ for every set $\Omega_k(r_d)$. The average over all sets $\Omega_k(r_d)$, normalized by the variance of the time series, σ_x , yields the target variance, $\sigma^{*2}(r_d)$:

$$\sigma^{*2}(r_d) = \frac{\frac{1}{N_0} \sum_{k=1}^{N_0} \sigma_k^2(r_d)}{\sigma_x^2}, \quad (6)$$

where N_0 denotes the total number of sets $\Omega_k(r_d)$.

5. Repeat steps 1 to 4 for the N_s surrogates.

Due to the standardization of the intervals of r_d , the DVV analysis can be conveniently illustrated in the resulting DVV plots, where the x-axis corresponds to the standardized distance r_d and the y-axis corresponds to the target variance. If the surrogate data yields similar results to that of the original signal, the target variance of the original signal falls within the confidence interval and the null hypothesis can not be rejected.

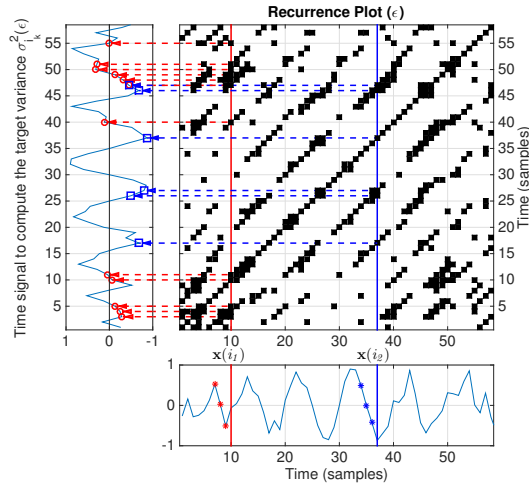
Those readers familiar with RPs can readily understand that the computation of the DVV plot can be explained by using RP concepts. The RP is a 2D plot that for a given moment in time shows the times at which a phase-space trajectory visits roughly the same area in the phase space.

Thus, for a given DV, using the RP, we can easily find the DVs that are closer than a given distance r_d just by looking in the corresponding column of the $\text{RP}(\varepsilon)$. The distance r_d is completely equivalent to the so-called ε in the RP (Eq. 2). Fig. 4 illustrates this idea and shows how we can obtain the corresponding set of targets (horizontal red and blue lines), $\Omega_k(r_d)$ in the DVV algorithm, for the later compu-

tation of its variance. Thus, for a given i_k and ε , we obtain $l_\varepsilon \subseteq \{j\}$ s.t. $R_{i_k j} = 1$, and $\sigma_{i_k}^2(\varepsilon) = \text{VAR}[x_{l_\varepsilon}]$, where $\text{VAR}[\cdot]$ is a variance estimator and x_{l_ε} is the target of the DV $\mathbf{x}(l_\varepsilon)$. Averaging this variance for N_0 different DVs and dividing by the variance of the time series (σ_x^2), we obtain Eq. (7) which is clearly equivalent to Eq. (6). Note that the plot of this normalized variance $\sigma^{*2}(\varepsilon)$ as a function of the standardized distance is the DVV plot.

$$\sigma^{*2}(\varepsilon) = \frac{\frac{1}{N_0} \sum_{k=1}^{N_0} \sigma_{i_k}^2(\varepsilon)}{\sigma_x^2} \quad (7)$$

Fig. 4 Example of how to find the nearest DVs and the normalized variance of its targets using $\text{RP}(\varepsilon)$. The red and blue vertical lines are two randomly chosen DVs ($\mathbf{x}(i_1)$ and $\mathbf{x}(i_2)$) using $m = 3$, $\tau = 1$) represented in the bottom panel using asterisks. The red and blue horizontal dashed lines are their corresponding neighbours that lie within the distance ε . The red circles in the left panel are the corresponding targets of $\mathbf{x}(i_1)$; the blue squares are the corresponding targets of $\mathbf{x}(i_2)$. The RP was computed for an ε corresponding to 14% of black points.



The analysis of target variance based on a distance r_d in the DVV algorithm, or a distance ε in the RP, is an indicator of the recurrence behavior of the studied phase space. This is not the only way to quantify the number and duration of recurrences of a dynamic system represented by its phase-space trajectory. A proper selection of a RQA measure allows an equivalent analysis that is less parameter dependent and that has greater robustness.

3.2 RQA measures as discriminating statistics

The recurrence plots exhibit characteristic large-scale and small-scale patterns that are caused by typical dynamic behaviour. The appearance of diagonal lines is related to a similar local evolution of different parts of the trajectory, whereas the appearance of vertical and horizontal black lines means that the trajectory does not change its state for some time [31]. Zbilut and Webber developed Recurrence Quantifica-

tion Analysis (RQA) to quantify a RP [32]. They define measures using the recurrence point density and the diagonal structures in the recurrence plot: the recurrence rate (RR), the determinism (DET), the maximal length of the diagonal structures, the entropy and the trend (see Table 1). The recurrent points delineate the number of embedded vector pairs that are near each other in the m -dimensional; however, the measures related to the diagonal patterns distinguish between points individually dispersed and those that represent parts of the signal where the signal similarly evolves. Gao et Al. [33, 34] carried out a detailed analysis about the reasons for the appearance of vertical lines (and horizontal lines for fixed values of ϵ) and its relation with the appearance of square-like textures in RPs. The underlying reasons for the abundance of vertical lines (and therefore square-like structures) are: i) the usage of a high sampling frequency (i.e., a small sampling time); and ii) the usage of a fairly large recurrence radius ϵ for constructing a RP. Based on this analysis, some recurrence time statistics corresponding to vertical structures were introduced. Marwan et Al. [31, 35] extended this view on the vertical structures and defined measures of complexity based on the distribution of the vertical line length: laminarity (LAM), trapping time (TT), and the maximal length of the vertical structures (see Table 1). Those variables have widely been applied to identify laminar states and their transitions between regular and chaotic regimes [36], as well as to detect the presence of unstable singularities which are often found in biological dynamics [31, 37].

The main purpose of the statistical test within the surrogate data method is to be sensitive to any changes that are exclusively related to the null hypothesis under study. For that reason, it is necessary to point out the need to understand the signal modality characteristic being studied and its relationship with the applied surrogate data generation algorithm.

As discussed in subsection 2.1, the hypothesis of non-linearity is linked to the presence of information in the phase spectrum. The randomization of the phase spectrum leads to significant changes in the structure of the signal. Even though the surrogates of a non-linear signal (using the WiAAFT algorithm) preserve the probability distribution and the spectrum amplitude (and therefore the autocorrelation function) of the original signal, they have a new arrangement of closest points. The DVV algorithm detects these changes through the variance of the targets of the closest points. An equivalent measure of RQA that is susceptible to the distribution of the closest points is the Trapping Time (TT), which is a statistic that is linked to the laminarity of a dynamic system. The study of the TT measure as a function of the recurrence threshold ϵ , $TT(\epsilon)$, allows the evolution of recurrent states to be studied as the percentage of nearby points increases. In the case of linear signals, the statistic vector computed for the surrogate data will coincide with the vector $TT(\epsilon)$ of the original signal. In the case of the non-linear data will not coincide, and this permits the non linear signals to be identified.

A similar argument can be made regarding the hypothesis of complexity using the PPTS algorithm (subsection 2.2) for oscillatory signals. When generating the surrogates, jumping among twin points breaks the diagonals when the signals deviate from a quasi-periodic oscillation. This produces surrogates with different diagonal

line lengths in the RP for temporal series having high complexity while maintaining approximately the same diagonal line lengths in quasi-periodic ones. An equivalent measure of RQA that is susceptible to the diagonal line length distribution is the average diagonal line length L , or any other measure related to the diagonal line length (see Table 1). The study of L as a function of the recurrence threshold ϵ , $L(\epsilon)$, and the comparison with that of its surrogates allows the complexity to be identified.

Note that in both analyses, the phase-space reconstruction for the original and the surrogates data must be done with the same embedding parameters, τ and m . Moreover, the statistics compared (the original signal and the surrogates) need to be computed with the same percentage of black points in the RP matrix. In this work, a sweep between 10 % and 80 % of the black points has been performed. This new representation (herein called DVRQA, Delay Vector Recurrence Quantification Analysis) eliminates the problem of choosing the most appropriate threshold for computing the RP in an unknown situation. Unlike the technique described above, which only takes into account some randomly chosen points, one of the advantages of statistical analysis based on RQA is that it uses the entire signal. This is supposed to be a more robust technique that is less parameter dependent and has smaller resultant confidence intervals. In addition, this technique eliminates the need for an estimator, such as the variance, that needs a high minimum number of points for a correct estimation.

The DVRQA analysis can be summarized as follows:

1. Compute the distance vector ϵ that produces a RP with a percentage of black points between 10% and 80% of the total number of points.
2. For each one of the elements in the vector ϵ , compute the RP (Eq. 2) and obtain the selected RQA measure based on the null-hypothesis under study. We refer to the RQA measure as $DVRQA_{orig}(\epsilon)$.
3. Repeat steps 1-2 for the N_s surrogates to establish the confidence intervals. The RQA measure for the i -th surrogate is now referred to as $DVRQA_{surr,i}(\epsilon)$.
4. Plot both variables on the same normalized graph. This will be referred as the DVRQA plot.

The computational complexity of the DVRQA analysis depends on the RQA measure selected. For simple RQA measures, the computational complexity can be similar to that of the DVV method. In more sophisticated measures, fast algorithms such as those described in [38] can be used.

Table 1 Some of the possible measures for the recurrence quantification analysis (RQA). [31, 32, 35]

SYMBOL	DESCRIPTION	EQUATION
<i>RR</i>	Recurrence rate: density of recurrence points.	$\frac{1}{N^2} \sum_{i,j=1}^N R_{i,j}$
<i>TT</i>	Averaged vertical line length. ^a	$\frac{\sum_{v=v_{min}}^N v \cdot P(v)}{\sum_{v=v_{min}}^N P(v)} \quad (8)$
<i>LAM</i>	Laminarity: Percentage of recurrence points that form vertical lines. ^a	$\frac{\sum_{v=v_{min}}^N v \cdot P(v)}{\sum_{v=1}^N v \cdot P(v)}$
<i>L</i>	Averaged diagonal line length. ^b	$\frac{\sum_{l=l_{min}}^N l \cdot P(l)}{\sum_{l=l_{min}}^N P(l)} \quad (9)$
<i>DET</i>	Determinism: Percentage of recurrence points that form diagonal lines. ^b	$\frac{\sum_{l=l_{min}}^N l \cdot P(l)}{\sum_{i,j=1}^N R_{i,j}}$

^a $P(v)$ is the histogram of the lengths v of the black diagonal lines, and v_{min} is the minimal length of what should be considered to be a vertical line (typically, $v_{min} = 2$).

^b $P(l)$ is the histogram of the lengths l of the black diagonal lines, and l_{min} is the minimal length of what should be considered to be a diagonal line (typically, $l_{min} = 2$).

3.3 Hypothesis Test

The modality tests done in this work compare different kinds of Recurrence Quantification measures that are computed for the original signal to those obtained for an ensemble of surrogates. So far in this work, only a visual comparison of the statistical measures studied for the original signal, $DVRQA_{orig}(\varepsilon)$, and the surrogates, $DVRQA_{surr,i}(\varepsilon)$ has been done. However, it is easy to implement a statistical test to quantify the level of similarity or difference that allow the hypothesis under study to be accepted or rejected.

The metric used in the analysis is the same as in the original DVV algorithm but substituting the variance estimator for each of the applied RQA measures, ξ , in each case:

$$t_\xi = \sqrt{\left\langle \left(\xi^2(\varepsilon) - \frac{\sum_{i=1}^{N_s} DVRQA_{surr,i}^2(\varepsilon)}{N_s} \right) \right\rangle_\varepsilon} \quad (10)$$

where $DVRQA_{surr,i}(\varepsilon)$ is the corresponding RQA metric at recurrence threshold ε for the i -th surrogate, and the average $\langle \cdot \rangle_\varepsilon$ is taken for each component of the threshold vector, ε . The variable ξ is replaced by $DVRQA_{orig}(\varepsilon)$ to compute the metric corresponding to the original signal, t_o , and replaced by $DVRQA_{surr,i}(\varepsilon)$ ($i = 1, \dots, N_s$) to compute the metric corresponding to each surrogate, $t_{s,i}$.

Since the analytical form of the probability distribution of the applied metric is not known, a non-parametric, rank-based test is used [39]. In this work, for every original time series, we generate $N_s = 99$ surrogates. The metric for the original signal, t_o , and for the surrogates, $t_{s,i}$ ($i = 1, \dots, N_s$), are computed, and the series $\{t_o, t_{s,i}\}$ is sorted in increasing order, after which the position index (rank) r of t_o is determined. A right-tailed test is rejected (and therefore the null hypothesis under study) if the rank r of the original time series exceeds 90. In this way, a single test statistic is obtained, and the above-mentioned right-tailed surrogate testing quantifies the level of rejection of the null hypothesis. In section 4, the results of the corresponding rank tests for the analyzed examples are presented.

4 Applications

This section presents some results of signal modality characterization for the detection of non-linearities and complexity using both the surrogate data generation algorithms presented in Section 2 and the test statistics based on RQA measures presented in Section 3.

The linear and non-linear nature of time series is examined by performing the DVRQA analysis on both the original and 99 surrogates time series computed with the WiAAFT algorithm. The statistical measure applied was the TT measure. To verify the proposed technique, a number of time series with different linear and non-linear natures were generated. Each of the generated signals consisted of 1000 samples. The first two signals correspond to the examples in the text seen so far: the quasiperiodic signal (Eq. 4) and the Rössler signal (Eq. 5). Two random signals were also studied: Model 1 (Eq. 11) and Model 2 (Eq. 12).

$$y_k = 0.3 + 0.7 \cdot y_{k-1} + v_k + 0.4 \cdot v_{k-1} \quad (11)$$

where $y_0 = 0$ and v_k is a standard normal distribution, $N(0, 1)$.

$$y_k = v_k + 0.8 \cdot v_{k-1} \cdot v_{k-2} \quad (12)$$

where v_k is a standard normal distribution, $N(0, 1)$. For each signal, the optimal embedding parameters were determined using the mutual algorithm and the Cao method.

The results of the DVRQA analysis are illustrated in Fig. 5. The first signal analyzed is the quasiperiodic signal (Fig. 5a). The computed TT vector for the original signal coincides with the results obtained for the surrogates. The resulting rank-test is equal to 34, and therefore the linear null hypothesis can not be rejected. Fig. 5b corresponds to the simulation of the Rössler signal, a well-known example of a chaotic (non-linear and deterministic) signal. In this case, the resulting TT values for the original signal significantly differ from the ones for the surrogates at both ends of the graph. The resulting value of the rank-order test, r , is 100, and the signal can be identified as non-linear. For the stochastic Model 1, the values of TT fall into the confidence interval defined by the surrogates (the rank-test equals to 65). However, in the case of the non-linear Model 2 (Fig. 5d), the original and surrogate statistics are clearly different. Undoubtedly, the variable r is equal to 100 and the null-hypothesis related to linearity can be rejected.

Note that for the continuous time systems (the quasiperiodic and the Rössler signals), the maximum value of the TT measure is higher than the one computed for the stochastic signals, Model 1 and Model 2. As stated above, the trapping time is closely related to the sampling time and the recurrence radius. High values of TT appear for continuous time systems with a high time resolution and with a re-

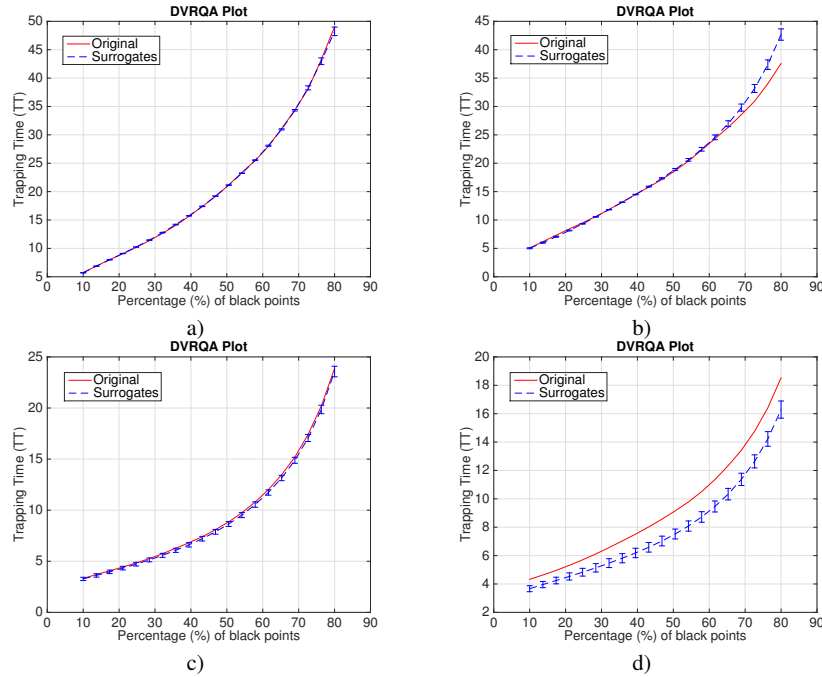


Fig. 5 DVRQA analysis with 99 WiAAFT surrogates performed on four simulated time series using the embedding parameters obtained via the mutual information algorithm (τ) and the Cao method (m): a) Quasiperiodic signal; b) Rössler signal; c) Model 1; and d) Model 2.

currence threshold ε that is not too small. However, the vertical structures are less prominent for maps and continuous systems that are reconstructed with small values of ε , unless the signals present any kind of singularities or intermittences [34, 31]. The DVRQA analysis based on the TT can also provide information about the laminarity of the phase space under study.

We are now going to illustrate how the proposed algorithms can be used in a real application for the characterization and detection of irregular animal vocalizations. We analyzed a recording containing dog barking sounds with different Harmonic to Noise Ratio (HNR). This parameter can be used in animal bioacoustics to quantify dysphonia. Normal sounding dogs occupy a middle HNR range, while dysphonic dogs exceed this range with higher as well as lower HNR values [40], [41]. To demonstrate this idea, we used a database from [42] which contains dysphonic sounds from animals that were recorded with a sample frequency of 22050 Hz.

Due to the oscillatory nature of the animal vocalizations and the fact that the appearance of this non-linear phenomenon results in the generation of an immeasurable number of new frequencies, it seems appropriate for the null hypothesis to be the measure of the complexity of each of the signals. The increase in complexity may indicate some kind of pathology [43]. Therefore, we propose the use of the PPTS algorithm and the average diagonal line length (L) to detect and characterize dysphonia phenomena.

Fig. 6 (top) shows the time representation of a medium HNR dog bark together with the phase-space representation (only the first two components of the DVs). Fig. 6 (bottom) shows the time representation of one of the computed PPTS together with its phase-space representation. It is important to note that the phase-space representation of both the original and one of the surrogates are quite similar.

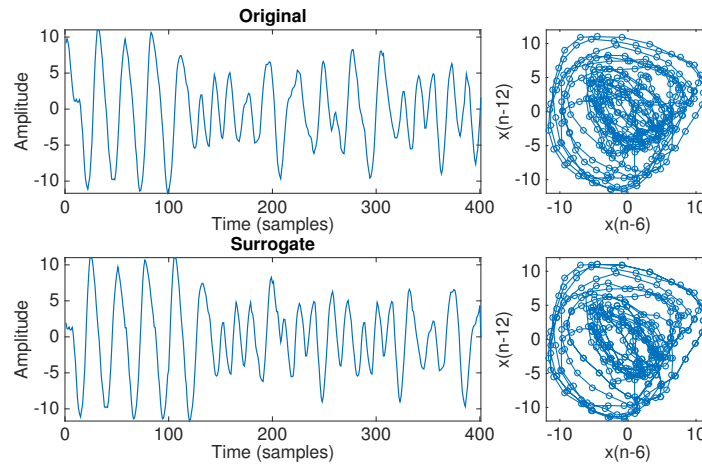


Fig. 6 Top: Time representation of the medium HNR dog sound alongside with its phase-space representation. Bottom: Time representation of one of the surrogates obtained with the PPTS together with its phase-space representation.

A DVRQA test was done to analyze the dog barking sounds. We chose the average diagonal line length (L) as the discriminating measure. This measure (and any other RQA measures related to diagonal line length) captures determinism or predictability and is therefore a good candidate for the null test hypothesis of deviation of a periodic or quasi-periodic oscillation. We analyzed three different dog barks with three different HNR values: low HNR, medium HNR, and high HNR. The panels on the left in Fig. 7 show the temporal series together with their corresponding time frequency representation. Only fragments of 400 samples were analyzed. The starting point for the selection of the DVRQA analysis is not crucial (we obtained very similar results independently of the initial position of the 400 samples window). The red vertical line indicates the exact point where the DVRQA analysis was done. The panels on the right of the Fig. 7 show the DVRQA tests for each one of the dog barks. The confidence intervals were obtained computing 99 PPTS for each example of dog barks. The null hypothesis is that the signal can be obtained as the sum of sinusoids with incommensurate frequencies.

The low and medium HNR dog barks are very difficult to distinguish by looking at their corresponding time frequency representations. However, the DVRQA plot allows a clear differentiation between these two sounds. The null hypothesis can not be rejected for the low HNR dog bark since the rank-test results in r equals to 1, meaning that the $DVRQA_{orig}$ almost exactly match with the average of its surrogates, $DVRQA_{surr,i}$ (the red line in Fig. 7b falls in the middle of the confidence interval). On the other hand, the hypothesis test for the medium HNR dog bark can be rejected with a value of the rank-order test, r , equals to 90. This can be used to help distinguish between normal and dysphonic dogs.

In the time frequency representation of the high HNR dog barks, it is easy to see the presence of frequencies that lie between or below the main harmonic frequencies. This is a non-linear phenomenon known as subharmonic generation that also appears in pathological voices. For the high HNR dog bark, the DVRQA plot clearly shows a deviation from a periodic or a quasiperiodic oscillation, and the null test can be rejected with the variable r equals to 100 in the confidence interval. It must be highlighted that RQA measures combined with the surrogate approach can characterize phenomena that are usually analyzed by means of time-frequency techniques.

5 Conclusions

In this work, we have analyzed the problem of using hypothesis testing for the non-linear detection and characterization of complexity in temporal series from the RPs point of view. In order to do this, we have focused on both the generation of surrogates and the design of new statistical tests. To generate surrogates, we worked with the WiAAFT algorithm, which is a technique that maintains the temporal structure of the original signal and at the same time provides a sufficient degree of randomness to obtain valid surrogates for testing non-linearity (which are suitable for non-

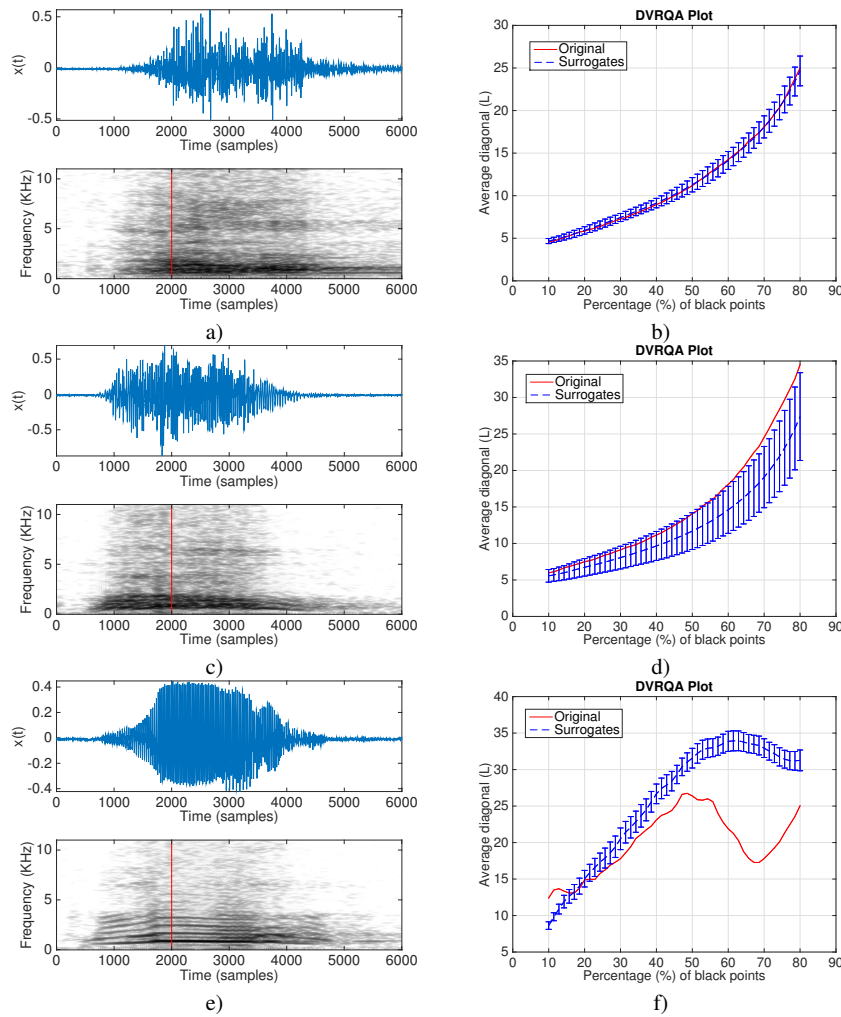


Fig. 7 a) TFR of a low HNR dog bark, b) DVRQA analysis of a low HNR dog bark, c) TFR of a medium HNR dog bark, d) DVRQA analysis of a medium HNR dog bark, e) TFR of a high HNR dog bark, f) DVRQA analysis of a high HNR dog bark. The red vertical line indicates where the DVRQA analysis was performed (99 PPTS were used for the analyses).

stationary signals). We have also created surrogates of a different kind, the PPTS, which are valid for detecting non-linear determinism and complexity in short oscillating signals. RPs play an important role both in the definition of twin points and the understanding of the PPTS algorithm. We have also demonstrated that RPs are not only a valid tool for the generation of surrogates but also for the design of the statistical tests. This has been illustrated by reformulating the DVV method using RPs.

This analysis has led to the creation of new discriminating tests that are based on RQA oriented to hypothesis testing (i.e., non-linear and complexity detection). The proposed test (DVRQA) has the advantage of analyzing the recurrent structures without having to choose the most appropriate recurrence threshold in an unknown situation. The selection of the RQA metrics must be carefully chosen based on the surrogates. The trapping time measure captures significant differences in the degree of locality and is therefore appropriate for testing non-linearity with the WiAAFT algorithm. The PPTS has proven to be useful for testing complexity in short oscillating signals using the averaged diagonal line length.

We have demonstrated through simulations that we can detect non-linearities in signals of different nature (stochastic and deterministic) using the proposed algorithms. Moreover, we have analyzed the problem of anomalies in the voice production of mammals and the use of algorithms for their detection and characterization. The analysis of a database containing real-world sounds from dysphonic dogs has shown that the L measure, together with the PPTS algorithm, allows the relationship among HNR, complexity and dysphonic dog barking sounds to be established. This technique has the potential to be applied in many other domains.

Acknowledgements This work has been supported by the Spanish Administration under grant TEC2011-23403.

References

1. K. Lehnertz, R. G. Andrzejak, J. Arnhold, T. Kreuz, F. Mormann, C. Rieke, A. Widman, and C. E. Elger. Nonlinear EEG analysis in epilepsy: its possible use for interictal focus localization, seizure anticipation, and prevention. *Journal of Clinical Neurophysiology: Official Publication of the American Electroencephalographic Society*, 18(3):209–222, 2001.
2. W. T. Fitch, J. Neubauer, and H. Herzel. Calls out of chaos: the adaptive significance of nonlinear phenomena in mammalian vocal production. *Animal Behaviour*, 63(3):407–418, 2002.
3. D. G. McMillan. Non-linear predictability of UK stock market returns. *Oxford Bulletin of Economics and Statistics*, 65(5):557–573, 2003.
4. F. Laio, A. Porporato, L. Ridolfi, and S. Tamea. Detecting nonlinearity in time series driven by non-Gaussian noise: the case of river flows. *Nonlinear Processes in Geophysics*, 11(4):463–470, October 2004.
5. P. Borgnat, P. Flandrin, P. Honeine, C. Richard, and J. Xiao. Testing stationarity with surrogates: A Time-Frequency approach. *IEEE Transactions on Signal Processing*, 58(7):3459–3470, July 2010.
6. M. Small and C. K. Tse. Detecting determinism in time series: the method of surrogate data. *IEEE Transactions on Circuits and Systems I: Fundamental Theory and Applications*, 50(5):663–672, May 2003.
7. J. Theiler, S. Eubank, A. Longtin, B. Galdrikian, and J. D. Farmer. Testing for nonlinearity in time series: the method of surrogate data. *Physica D: Nonlinear Phenomena*, 58(1):77 – 94, 1992.
8. T. Schreiber and A. Schmitz. Improved surrogate data for nonlinearity tests. *Physical Review Letters*, 77(4):635–638, 1996.
9. X. Luo, T. Nakamura, and M. Small. Surrogate test to distinguish between chaotic and pseudoperiodic time series. *Physical Review E*, 71(2), February 2005.

10. T. Nakamura and M. Small. Small-shuffle surrogate data: Testing for dynamics in fluctuating data with trends. *Physical Review E*, 72(5):056216, 2005.
11. M. Small, D. Yu, and R. Harrison. Surrogate test for pseudoperiodic time series data. *Physical Review Letters*, 87(18), 2001.
12. M. Thiel, M. C. Romano, J. Kurths, M. Rolfs, and R. Kiegl. Twin surrogates to test for complex synchronisation. *Europhysics Letters*, 75(4):535–541, August 2006.
13. M. C. Romano, M. Thiel, J. Kurths, K. Mergenthaler, and R. Engbert. Hypothesis test for synchronization: Twin surrogates revisited. *Chaos*, 19(1):015108, 2009.
14. T. Schreiber and A. Schmitz. Improved surrogate data for nonlinearity tests. *Phys. Rev. Lett.*, 77:635–638, Jul 1996.
15. D. Kaplan. Nonlinearity and Nonstationarity: The Use of Surrogate Data in Interpreting Fluctuations. *Proceedings of the 3rd Annual Workshop on Computer Applications of Blood Pressure and Heart Rate Signals*, 1997.
16. M. C. Casdagli and A. S. Weigend. *Exploring the continuum between deterministic and stochastic modeling, in Time Series Prediction: Forecasting the Future and Understanding the Past*. Reading, MA: Addison-Wesley. 1994.
17. T. Gautama, D. P. Mandic, and M. M. Van Hulle. The delay vector variance method for detecting determinism and nonlinearity in time series. *Physica D: Nonlinear Phenomena*, 190(3-4):167–176, April 2004.
18. N. H. Packard, J. P. Crutchfield, j. D. Farmer, and R. S. Shaw. Geometry from a time series. *Physical review letters*, 45(9):712, 1980.
19. D. P. Mandic, M. Chen, T. Gautama, M. M. Van Hulle, and A. Constantinides. On the characterization of the deterministic/stochastic and linear/nonlinear nature of time series. *Proceedings of the Royal Society A: Mathematical, Physical and Engineering Sciences*, 464(2093):1141–1160, 2008.
20. A. Fraser and H. Swinney. Independent coordinates for strange attractors from mutual information. *Phys. Rev. A*, 33:1134–1140, Feb 1986.
21. M. B. Kennel, R. Brown, and H. D. I. Abarbanel. Determining embedding dimension for phase-space reconstruction using a geometrical construction. *Phys. Rev. A*, 45:3403–3411, Mar 1992.
22. L. Cao. Practical method for determining the minimum embedding dimension of a scalar time series. *Physica D: Nonlinear Phenomena*, 110(12):43 – 50, 1997.
23. J. P. Eckmann, S. Kamphorst, S. Oliffson, and D. Ruelle. Recurrence plots of dynamical systems. *Europhys. Lett*, 4(9):973–977, 1987.
24. C. J. Keylock. Improved preservation of autocorrelative structure in surrogate data using an initial wavelet step. *Nonlinear Processes in Geophysics*, 15(3):435–444, June 2008.
25. D. B. Percival and A. T. Walden. *Wavelet Methods for Time Series Analysis (Cambridge Series in Statistical and Probabilistic Mathematics)*. Cambridge University Press, February 2000.
26. C. Tao and J. J. Jiang. Chaotic component obscured by strong periodicity in voice production system. *Physical Review E*, 77:061922, Jun 2008.
27. R. Miralles, L. Vergara, A. Salazar, and J. Igual. Blind detection of nonlinearities in multiple-echo ultrasonic signals. *IEEE Transactions on Ultrasonics, Ferroelectrics, and Frequency Control*, 55,3:1–11, March 2008.
28. R. Miralles, A. Carrion, D. Looney, G. Lara, and D. Mandic. Characterization of the complexity in short oscillating time series: An application to seismic airgun detonations. *The Journal of the Acoustical Society of America*, 138(3):1595–1603, September 2015.
29. M. T. Rosenstein, J. J. Collins, and C. J. De Luca. A practical method for calculating largest Lyapunov exponents from small data sets. *Physica D: Nonlinear Phenomena*, 65(1-2):117–134, May 1993.
30. P. Grassberger and I. Procaccia. Measuring the strangeness of strange attractors. *Physica D: Nonlinear Phenomena*, 9(1-2):189–208, October 1983.
31. N. Marwan, N. Wessel, U. Meyerfeldt, A. Schirdewan, and J. Kurths. Recurrence-plot-based measures of complexity and their application to heart-rate-variability data. *Physical review E*, 66(2):026702, 2002.

32. C. L. Webber and J. P. Zbilut. Dynamical assessment of physiological systems and states using recurrence plot strategies. *Journal of Applied Physiology*, 76(2):965–973, 1994.
33. J. B. Gao. Recurrence time statistics for chaotic systems and their applications. *Phys. Rev. Lett.*, 83:3178–3181, Oct 1999.
34. J. Gao and H. Cai. On the structures and quantification of recurrence plots. *Physics Letters A*, 270(12):75 – 87, 2000.
35. N. Marwan, M. C. Romano, M. Thiel, and J. Kurths. Recurrence plots for the analysis of complex systems. *Physics Reports*, 438(5):237–329, 2007.
36. K. Klimaszewska and J.J. Żebrowski. Detection of the type of intermittency using characteristic patterns in recurrence plots. *Phys. Rev. E*, 80:026214, Aug 2009.
37. J. P. Zbilut and C. L. Webber Jr. Laminar recurrences, maxline, unstable singularities and biological dynamics. *The European Physical Journal Special Topics*, 164(1):55–65, 2008.
38. Tobias Rawald, Mike Sips, Norbert Marwan, and Doris Dransch. Fast Computation of Recurrences in Long Time Series. *Translational Recurrences, Springer Proceedings in Mathematics & Statistics*, 103:17–29, 2014.
39. J. Theiler and D. Prichard. Constrained-realization Monte-Carlo method for hypothesis testing. *Physica D: Nonlinear Phenomena*, 94(4):221 – 235, 1996.
40. T. Riede, H. Herzel, K. Hammerschmidt, L. Brunberg, and G. Tembrock. The harmonic-to-noise ratio applied to dog barks. *The Journal of the Acoustical Society of America*, 110(4), 2001.
41. T. Riede, B. R. Mitchell, I. Tokuda, and M. J. Owren. Characterizing noise in nonhuman vocalizations: Acoustic analysis and human perception of barks by coyotes and dogs. *The Journal of the Acoustical Society of America*, 118(1), 2005.
42. T. Riede. *Vocal changes in animals during disorders*. PhD. report. Mathematisch-Naturwissenschaftlichen Fakultät I der Humboldt-Universität zu Berlin. 2000. <http://edoc.hu-berlin.de/dissertationen/riede-tobias-2000-06-26/HTML/>.
43. I. Wilden, H. Herzel, G. Peters, and G. Tembrock. Subharmonics, biphonation, and deterministic chaos in mammal vocalization. *Bioacoustics*, 9(3):171–196, January 1998.